Journal of Cranio-Maxillo-Facial Surgery 47 (2019) 127–137

Contents lists available at ScienceDirect

Journal of Cranio-Maxillo-Facial Surgery

journal homepage: www.jcmfs.com

Real-time augmented model guidance for mandibular proximal segment repositioning in orthognathic surgery, using electromagnetic tracking

Sang-Jeong Lee [a, 1], Hoon Joo Yang [b, 1], Min-Hyuk Choi [a], Sang-Yoon Woo [a], Kyung-Hoe Huh [c], Sam-Sun Lee [c], Min-Suk Heo [c], Soon-Chul Choi [c], Soon Jung Hwang [d, **], Won-Jin Yi [a, c, *]

[a] Department of Biomedical Radiation Sciences (Head: Sung-Joon Ye, PhD), Graduate School of Convergence Science and Technology, Seoul National University, South Korea
[b] Orthognathic Surgery Center (Head: Soon Jung Hwang, DDS, MD, PhD), Seoul National University Dental Hospital, South Korea
[c] Department of Oral and Maxillofacial Radiology (Head: Min-Suk Heo, DDS, PhD), School of Dentistry and Dental Research Institute, Seoul National University, South Korea
[d] Department of Oral and Maxillofacial Surgery (Head: Jin-Young Choi, DDS, MD, PhD), School of Dentistry, Dental Research Institute, BK21 Plus, Seoul National University, South Korea

ARTICLE INFO

Article history:
Paper received 10 August 2018
Accepted 18 October 2018
Available online 26 October 2018

Keywords:
Orthognathic surgery
Mandibular proximal segment repositioning
Registration body
Augmented model-guided surgery
Tracking tool frame
Electromagnetic tracking tool

ABSTRACT

It is essential to reposition the mandibular proximal segment (MPS) as close to its original position as possible during orthognathic surgery. Conventional methods cannot pinpoint the exact position of the condyle in the fossa in real time during repositioning. In this study, based on an improved registration method and a separable electromagnetic tracking tool, we developed a real-time, augmented, model-guided method for MPS surgery to reposition the condyle into its original position more accurately.

After virtual surgery planning, using a complex maxillomandibular model, the final position of the virtual MPS model was simulated via 3D rotations. The displacements resulting from the MPS simulation were applied to the MPS landmarks to indicate their final postoperative positions. We designed a new registration body with 24 fiducial points for registration, and determined the optimal point group on the registration body through a phantom study. The registration between the patient's CT image and physical spaces was performed preoperatively using the optimal points.

We also developed a separable frame for installing the electromagnetic tracking tool on the patient's MPS. During MPS surgery, the electromagnetic tracking tool was repeatedly attached to, and separated from, the MPS using the separable frame. The MPS movement resulting from the surgeon's manipulation was tracked by the electromagnetic tracking system. The augmented condyle model and its landmarks were visualized continuously in real time with respect to the simulated model and landmarks.

Our method also provides augmented 3D coronal and sagittal views of the fossa and condyle, to allow the surgeon to examine the 3D condyle–fossa positional relationship more accurately. The root mean square differences between the simulated and intraoperative MPS models, and between the simulated and postoperative CT models, were 1.71 ± 0.63 mm and 1.89 ± 0.22 mm respectively at three condylar landmarks. Thus, the surgeons could perform MPS repositioning conveniently and accurately based on real-time augmented model guidance on the 3D condyle positional relationship with respect to the glenoid fossa, using augmented and simulated models and landmarks.

* Corresponding author. Department of Oral and Maxillofacial Radiology and Dental Research Institute, School of Dentistry, Seoul National University, Seoul, South Korea. Fax: +82 2 744 3919.
** Corresponding author. Department of Oral and Maxillofacial Surgery and Dental Research Institute, School of Dentistry, Seoul National University, Seoul, South Korea. Fax: +82 2 766 4948.
E-mail addresses: sjhwang@snu.ac.kr (S.J. Hwang), wjyi@snu.ac.kr (W.-J. Yi).
[1] contributed to this paper equally as first co-authors.

https://doi.org/10.1016/j.jcms.2018.10.016
1010-5182/

1. Introduction

In orthognathic surgery, the preoperative plan must be accurately transferred to the intraoperative procedure in order to accomplish a successful surgical outcome. During sagittal split ramus osteotomy (SSRO) surgery, the mandibular proximal segment (MPS) is repositioned to move the condyle to the correct position in the fossa (Epker et al., 1986). It is very important to locate the MPS as close to its original position as possible during the surgery (Costa et al., 2008). Dislocation of the condyle from the fossa during surgery can lead to immediate skeletal relapse, whilst posterior positioning of the condyle can cause condylar resorption, resulting in late relapse (Ellis et al., 1991; Hoppenreijs et al., 1999; Hwang et al., 2004). MPS rotation or excessively dislocated condyles in the fossa might also cause late skeletal relapse (Komori et al., 1989; Politi et al., 2004). Surgery-related changes in the condylar position might cause early or late occlusal instability and temporomandibular joint (TMJ) dysfunctions (Hu et al., 2000; Panula et al., 2000; Wolford et al., 2003). To overcome those problems, various techniques for repositioning the MPS into its preoperative position have been used, including splints (Landes et al., 2003), repositioning templates (Harada et al., 1994; Abou-ElFetouh et al., 2011), face bow recordings (Chow et al., 1985), and condylar positional devices (Gerressen et al., 2006, 2007). However, none of those methods can provide the exact position of the condyle in the fossa in real time during surgery.

Surgical navigation methods based on optical tracking have been introduced to transfer the surgical plan to the patient accurately during orthognathic surgery (Bettega et al., 1996, 2002; Bettega, Leitner, 2013; Nijmeh et al., 2005; Marmulla et al., 2007; Strong et al., 2008; Eggers et al., 2009; Zhang et al., 2011, 2012; Seeberger et al., 2012; Kim et al., 2013, 2014; Li et al., 2014; Lee et al., 2016; Savoldelli et al., 2018). The current surgical navigation system can optimize functional and aesthetic outcomes in patients with dentofacial deformities by identifying anatomical structures, transferring the surgical plan to the patient, and verifying the surgical results (Bobek, 2014). An early application of this surgical navigation system visualized the position of the pointing tool and the relative distance to the surgical target in the patient's body in real time (Eggers et al., 2009). 3D-rendered virtual bone-segment models were continuously tracked and visualized on the screen of the navigation system to provide intuitive perceptions of the surgical target and adjacent anatomical structures during surgery (Strong et al., 2008; Kim et al., 2014; Li et al., 2014; Lee et al., 2016). To overcome the disadvantages of the increased operational time and complexity caused by intraoperative registration, a preoperative registration technique was then applied to orthognathic surgery using a registration body (Kim et al., 2014; Lee et al., 2016). A virtual maxillomandibular complex (MMC) model was visualized, and the deviation errors between the current and preoperatively simulated landmark positions were quantified during repositioning in bimaxillary orthognathic surgery (Lee et al., 2016). However, the optical tracking-based navigation system suffered from line of sight obstruction between the tracking tool and camera, and the requirement for bulky tracking tools in local or minimally invasive surgeries (Lutz et al., 2015).

A navigation surgery system based on electromagnetic tracking has no line of sight problem and uses relatively small tracking tools, so it can be used in minimally invasive surgeries and to track internal organs (Seeberger et al., 2012; Berger et al., 2015, 2018; Lutz et al., 2015; Nova et al., 2017). The feasibility of applying this electromagnetic tracking system to maxillofacial surgery was verified in a study using a phantom skull under reproducible operating room conditions (Seeberger et al., 2012). Then, surgical navigation using the electromagnetic tracking system was applied to phantom trials for maxilla (Berger et al., 2015; Lutz et al., 2015) and MPS repositioning (Nova et al., 2017). In a previous study using electromagnetic surgical navigation for MPS repositioning, the electromagnetic tracking tool was fixed securely and inseparably to the bone segment (Berger et al., 2018), but that meant that the tracking tool itself and the wire connecting the tracking tool with the tracking system could interfere with the surgery or be broken during surgical procedures such as osteotomies and bone removal, which would increase the surgical time and effort, and could cause iatrogenic accidents (Berger et al., 2018).

In our previous study, we developed a model- and landmark-guided orthognathic surgical navigation system based on an optical tracking method that used virtual skeletal models made for each patient (Lee et al., 2016). This method, which used a virtual MMC model, provided accurate and flexible guidance during bimaxillary orthognathic surgery through intraoperative visualization and deviation quantification from the MMC model and landmarks (Lee et al., 2016). For the present study, we developed a real-time, augmented model-guided method for MPS surgery to reposition the condyle into its original position more accurately, based on an improved registration method and an electromagnetic tracking tool.

2. Materials and Methods

2.1. Acquisition of patient CT and 3D dentition images

The patient CT image was acquired using an MDCT (SOMATOM Sensation 10, Siemens, Munich, Germany) under 120 kVp and 80 mAs conditions, with a slice thickness of 0.75 mm. The patient underwent a CT scan with a dental splint attached to a reusable registration body (Kim et al., 2014; Lee et al., 2016). The patient dental splint was made from orthodontic self-curing acrylic resin (Ortho-Jet; Lang Dental Manufacturing Co, Wheeling, IL, USA). During CT scanning, the registration body was attached to the splint using a LEGO block (LEGO Group, Billund, Denmark). After the operation, the patient underwent an additional CT scan to evaluate the accuracy of the surgery postoperatively.

The patient's dental plaster casts were scanned using an optical model scanner (Maestro 3D, Maestro, Pisa, Italy) to obtain an artifact-free, high-resolution model of the maxillary and mandibular dentitions (Nkenke et al., 2004; Sohmura et al., 2004; Uechi et al., 2006; Frisardi et al., 2011; Naether et al., 2012; Lee et al., 2016). The final occlusal model of the postoperative maxillomandibular relationship was obtained by scanning the maxillary and mandibular dental casts positioned in the post-surgery maxillomandibular relation (Lee et al., 2016).

2.2. Determination of the optimal point group using a registration body

We designed a new registration body using CAD software and fabricated it with a 3D printer. The registration body was made as a symmetrical arch covering the bilateral MPSs, as close to the mandible as possible (Fig. 1). It consisted of two parts: an upper part with 24 holes of different depths and in different positions, containing ceramic balls 1 mm in diameter, for use as fiducial points for registration; and a lower part for installing the electromagnetic tracking tool (Fig. 1). At the lower part of the body, a LEGO block (LEGO Group, Billund, Denmark) was attached so that the registration body could be attached to the dental splint in the same positional relationship used previously for CT scanning during registration.

We used an electromagnetic tracking system (Aurora, Northern Digital Inc., Waterloo, Ontario, Canada) to track the 3D position of

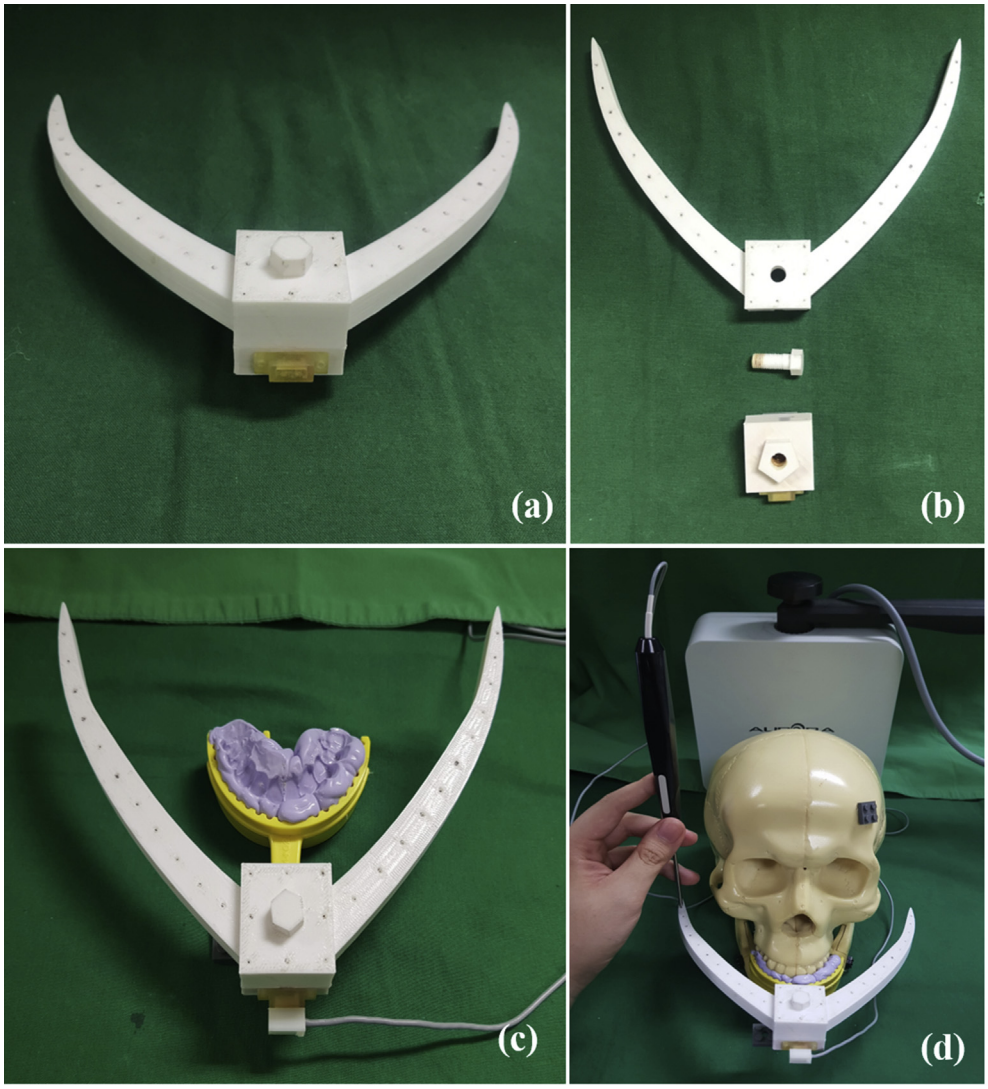

Fig. 1. The registration body consists of two parts: (a) an upper part with 24 ceramic ball fiducials and (b) a lower part for an electromagnetic tracking tool. (c) The registration body combined with the dental splint. (d) The fiducial position measurement with a tracked pointing tool was used with respect to the electromagnetic tracking tool on the body.

the MPS tracking tool in the phantom's physical space. The registration between the CT image and the physical spaces was performed by point-to-point matching, using six fiducial points on the registration body. The physical positions of the fiducial balls on the registration body were measured using a tracked pointing tool with respect to the electromagnetic tracking tool on the body (Fig. 1(c) and (d)). The measured physical positions were then matched to the corresponding positions on the 3D CT image space. The affine transformation between the patient's physical coordinates and the CT image coordinate system was derived as a result of the registration (M_{reg} in Equation (1)). Because the registration body (attached to the electromagnetic tracking tool) was always at the same fixed position on the splint, the physical positions of the fiducials recorded previously could be reused without remeasuring. That is, the registration could be performed using the registration body fiducials preoperatively.

Using a phantom study we determined the optimal point group on the registration body for registration between the patient's CT image and the physical spaces. We placed seven ceramic balls (1 mm in diameter) on the left and right MPS of a phantom skull to evaluate the accuracy of the registration body (Fig. 2(a) and (b)). The true positions of the ceramic ball points were measured in the phantom's CT image space before the experiment. After registration, the physical positions of the ceramic balls on the MPS were measured with respect to the reference tracking tool on the phantom skull by directly applying a tracked pointing tool to the balls (Fig. 2(c)). Then the physical positions of the ceramic balls were transformed into position in the CT image space using Equation (1):

$$T_{PS\_image} = M_{reg}\left(T_{ref\_init}^{-1} T_{PS\_init}\right)^{-1} T_{ref\_physical}^{-1} T_{PS\_physical} \quad (1)$$

where $T_{PS\_physical}$ is the current position of the MPS tracking tool, $T_{ref\_physical}$ is the current position of the reference tracking tool, T_{PS_init} is the initial position of the MPS tracking tool, and T_{ref_init} is the initial position of the reference tracking tool.

To determine the optimal fiducial points for registration, we made five combination groups from 24 fiducial points (Table 1). To quantify the accuracy of the groups, we calculated the root mean square (RMS) and the absolute difference between the measured and true positions of the balls on the MPS.

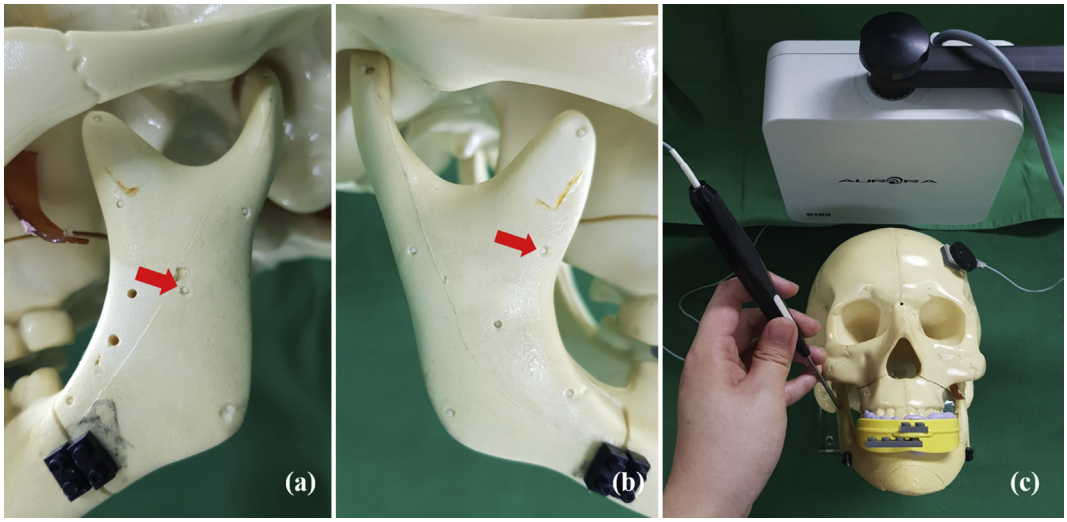

Fig. 2. Ceramic ball landmarks placed on the left MPS (a) and right MPS (b) of the phantom. (c) Measurement of the physical positions of the landmarks (by arrows) with respect to the reference tracking tool on the skull after registration using an electromagnetic tracking system.

Table 1
Five groups of fiducial point combinations used to determine the registration accuracy.

	Left anterior	Left posterior	Right anterior	Right posterior
Group 1	6	0	0	0
Group 2	0	6	0	0
Group 3	0	0	6	0
Group 4	0	0	0	6
Group 5	0	3	0	3

2.3. Simulation models produced by surgery planning for MPS repositioning

The surface models of the patient skull were generated by applying the marching cube algorithm to the CT image data. The virtual maxillary, mandibular, MPS, and other skeletal models were produced from the CT skull model by cutting according to the plane used in the actual surgery. The scanned dentition models were fused with the maxillary and mandibular CT models by registration, using an ICP algorithm. The virtual MMC model was also generated by two successive registrations of the maxillary and mandibular models with the final occlusion model, representing the simulated postoperative maxillomandibular relationship.

Virtual planning of the orthognathic surgery was performed by applying the desired amount of displacement to the landmarks, which we selected directly on the teeth of the virtual maxillary model (Kim et al., 2014; Lee et al., 2016). After the virtual surgery planning using the maxilla model, we applied the resulting displacements to the virtual MMC model to simulate the final position of the MMC. After the MMC planning, we simulated the final position of the MPS model mainly by 3D rotations. We determined the center of rotation using the condylion. The MPS model was rotated towards the distal segment so that there was intersegmental bony interference to be removed surgically, and the bilateral frontal ramal inclinations were similar. The MPS model was repositioned mainly by rolling, with yawing performed as needed to make contact with the distal segment under adequate frontal ramal inclination. When the inferior border of the proximal segment was located below the distal segment after repositioning, counterclockwise rotation was performed to even up the inferior border. However, clockwise rotation was not performed in the opposite case. Before the MPS simulation, we selected three anatomical landmarks at the condyle and one at the angle of the mandible, and applied the displacements from the MPS simulation to those landmark positions, simulating their final postoperative positions. We later used those landmarks to quantify the deviation error between the intraoperative and simulated positions of the MPS during surgery.

2.4. Intraoperative visualization and quantification of condyle repositioning in real time, based on augmented models and using a separable electromagnetic tracking tool

To track the patient's MPS electromagnetically we used a 3D printer to develop a frame that installed the electromagnetic tracking tool on the MPS. The frame consisted of two separable parts: one part ($20 \times 6 \times 5$ mm) fixed the frame itself to the MPS bone using screws; the other part ($12 \times 6 \times 6$ mm) was used to insert or detach the electromagnetic tracking tool (Fig. 3). Complementary shapes meant that the tracking tool could be combined with the fixed part in only one position and orientation. As a result, the electromagnetic tracking tool and the MPS bone were always combined in the same geometrical relationship during surgery.

The whole procedure for the real-time, augmented, model-guided MPS reposition is as follows (Fig. 4). Preoperative registration was performed to match the patient's physical and CT image spaces using the optimal fiducial points determined previously. The transformation was derived using the registration between the patient's physical and CT spaces (M_{reg} in Equation (1)). Before starting surgery, a reference electromagnetic tracking tool was fixed to the patient's skull to exclude errors caused by patient head movements during surgery. When the lower part of the registration body with the electromagnetic tracking tool was attached to the splint on the patient's dentition, the intraoperative registration process was completed immediately using the preoperative registration result (Kim et al., 2014; Lee et al., 2016). Then, the relative position of the tracking tool at the reference was recorded with respect to the splint tracking too,l so that the reference tool could be used as a reference point in the subsequent tracking.

During surgery, the splint with the registration body was removed from the patient. For the MPS repositioning surgery, the frame of the MPS tracking tool was installed firmly in the correct position on the MPS using screws, and the tracking tool removed from the splint was attached to the frame on the MPS by insertion. Then, the initial position of the tracking tool on the MPS was

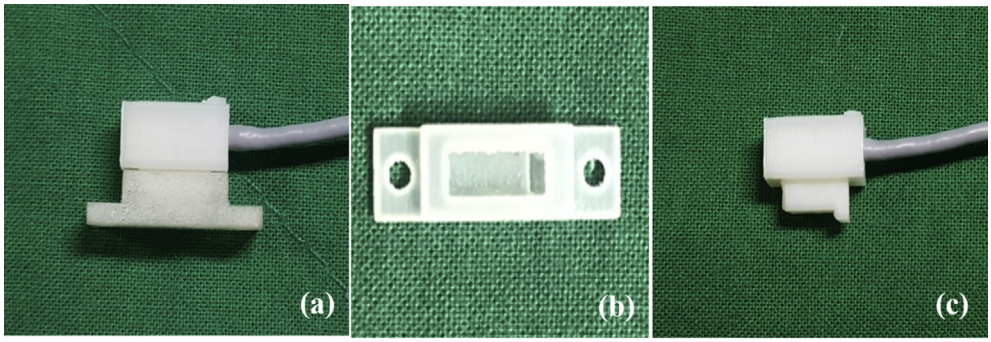

Fig. 3. The frame for installing the electromagnetic tracking tool on the MPS (a) consisted of two separable parts, one for fixing the frame itself onto the MPS bone (b) and the other for inserting and removing the electromagnetic tracking tool (c).

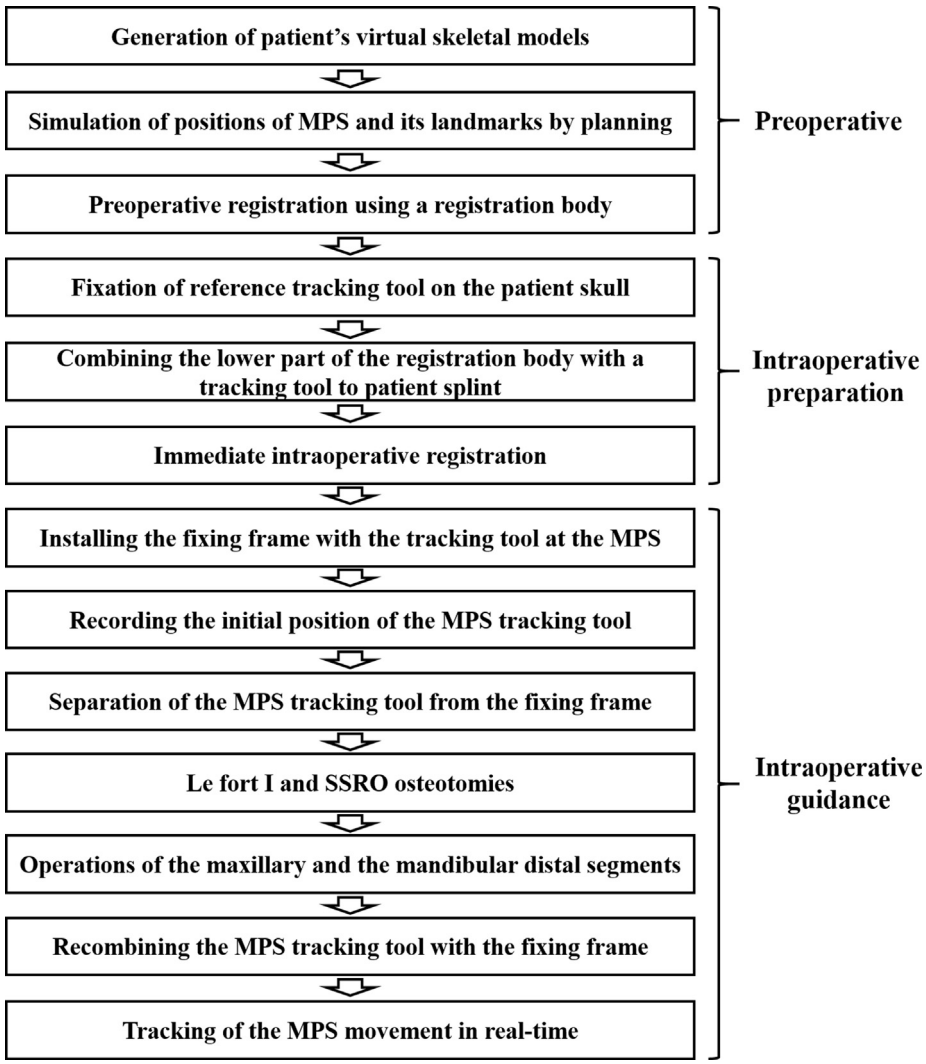

Fig. 4. The whole procedure for the real-time, virtual model–guided MPS repositioning.

recorded for later use. After this preparation, the MPS tracking tool was separated from the frame for the maxillary (Le Fort I) and mandibular (SSRO) osteotomies. After finishing the operations on the maxillary and mandibular distal segments, the MPS tracking tool was reinserted into the frame on the MPS in the same geometrical relationship used before. As the surgeon then moved the MPS, the movement was tracked by the electromagnetic tracking system (Aurora, Northern Digital Inc., Waterloo, Ontario, Canada). The augmented 3D condyle model was generated in real time with respect to the glenoid fossa during the MPS repositioning. The augmented condyle model and its landmarks were visualized continuously with respect to the simulated model and

landmarks while the MPS was being moved with a surgical instrument operated by the surgeon (Equation (1)). For intraoperative visualization and quantification in guiding the MPS repositioning, we used the same algorithm developed in our previous study (Kim et al., 2013, 2014; Lee et al., 2016).

After the orthognathic surgery, the patient's postoperative CT image was obtained under the same conditions used for the preoperative CT image. To evaluate the accuracy of the MPS reposition, the postoperative CT model was registered with the simulated MPS model produced by planning. The RMS and absolute differences between the simulated and postoperative positions of the landmarks on the MPS were calculated using the same anatomical landmarks used for intraoperative quantification. The errors at the landmarks were then analyzed statistically with ANOVA.

3. Results

To determine the optimal group of fiducial points on the registration body (Table 1), registration accuracy was calculated at the MPS landmarks on the phantom. Table 2 shows the absolute differences in the *x*, *y*, and *z* axes, and the RMS difference between the measured and true positions of the landmarks on the left and right MPSs. For the left MPS, the optimal point group was the second one, where the fiducial points were distributed on the posterior part of the left wing. The mean absolute value differences for the optimal point set were 0.49 ± 0.25, 0.18 ± 0.12, and 0.33 ± 0.32 mm on the x, y, and z axes, respectively, and the mean RMS difference was 0.68 ± 0.29 mm. For the right MPS, the optimal point group was the fourth one; the mean absolute differences were 0.56 ± 0.29, 0.30 ± 0.18, and 0.18 ± 0.15 mm on the *x*, *y*, and *z* axes, respectively, and the mean RMS difference was 0.72 ± 0.21 mm.

A 23-year-old female patient presented with dentofacial deformity (class III facial profile). The maxillary and mandibular models of the patient were fused with high-resolution, artifact-free dentition. The virtual maxillary, mandibular distal, MPS, and other skeletal models were produced by cutting (Fig. 5(a) and (b)). According to conventional paper surgery, the virtual surgery planning was performed by applying the required displacements to the dental landmarks. The resulting rotational movements of the maxillary model were 4.5 and 2.0 mm at the anterior pitch and posterior pitch, respectively. The translational movements were 1.0 mm on both the *x* and *y* axes. The total 3D displacement for the maxillary model was applied to the virtual MMC model to simulate the postoperative MMC model (Fig. 5(c) and (d)). The total 3D displacement for the postoperative MPS simulation (Fig. 5(c) and (d)) was applied to the MPS guidance landmarks, which also simulated the postoperative positions of the MPS landmarks (Fig. 6).

The planning result for the MPS reposition was transferred to the patient through image guidance using the virtual models. The electromagnetic reference tracking tool was fixed to the patient's skull. The lower part of the registration body, containing another electromagnetic tracking tool, was attached to the splint on the patient's dentition. The intraoperative registration process was then finished immediately using the preoperative registration result, and the splint with the registration body was removed from the patient's dentition. Next, the frame for the MPS tracking was firmly installed on the MPS using titanium screws (Fig. 7(a)), and the tracking tool removed from the splint was attached to the frame on the MPS by insertion (Fig. 7(b)). The initial position of the tracking tool on the MPS was recorded for use in the tracking to follow, and the tracking tool was separated from the frame for the maxillary (Le Fort I) and mandibular (SSRO) osteotomies.

After finishing the operations on the maxillary and mandibular distal segments, the MPS was recombined with the tracking tool and moved manually with a notched periosteal elevator controlled by a surgeon to reposition the MPS to the planned position (Fig. 7(c)). The intraoperative movement of the MPS during the operation was tracked continuously by the electromagnetic tracking system, and the augmented condyle model was visualized simultaneously on the screen. The current MPS model was visualized with the planned model in a different color (Fig. 8(a)). The current and planned landmarks were also visualized in different colors on the augmented models (Fig. 8(a)). The positional errors between the current and planned positions at the landmarks were calculated and visualized (Fig. 8(a)). To provide more intuitive information to the surgeon, the landmarks on the MPS model were shown in another color when the model approached the planned position closely (Fig. 8(a)) (Lee et al., 2016). Our method also provided augmented 3D coronal and sagittal views of the fossa and condyle to enable the surgeon to recognize the 3D condyle–fossa positional relationship accurately during the reposition (Fig. 8(b) and (c)). The surgeon could select one of the two views as needed and recognize the intraoperative position of the condyle inside the fossa intuitively. As a result, the 3D condyle position and its landmarks were visualized with respect to the glenoid fossa in real time during the MPS repositioning.

Immediately after finishing the MPS repositioning, the mean absolute differences between the simulated and intraoperative MPS models were 1.51 ± 0.44, 0.64 ± 0.58, and 1.03 ± 0.56 mm on the *x*, *y*, and *z* axes, respectively, and the mean RMS difference was 1.94 ± 0.76 mm at four landmarks on the MPS (Table 3). At three condylar landmarks, the mean absolute differences were 1.32 ± 0.42, 0.36 ± 0.15, and 0.89 ± 0.59 mm on the *x*, *y*, and *z* axes, respectively, and the mean RMS difference was 1.71 ± 0.63 mm. After surgery, the final accuracy was calculated by comparing the differences at the same landmarks on the simulated and postoperative MPS models. At four landmarks on the MPS, the mean absolute differences were 1.18 ± 0.61, 1.06 ± 1.17, and 1.46 ± 0.13 mm on the *x*, *y*, and *z* axes, respectively, and the mean RMS difference was 2.32 ± 0.88 mm (Table 3). At three condylar landmarks, the mean absolute differences were 0.94 ± 0.48, 0.49 ± 0.36, and 1.49 ± 0.14 mm on the *x*, *y*, and *z* axes, respectively, and the mean RMS difference was 1.89 ± 0.22 mm. The RMS

Table 2
Absolute differences in the *x*, y, and *z* axes and root mean square (RMS) differences between the true and measured positions of the landmarks on the bilateral MPS of the phantom after registration.

	Left MPS (mm)				Right MPS (mm)			
	x	*y*	*z*	RMS	*x*	*y*	*z*	RMS
Group 1	0.65 ± 0.34	0.69 ± 0.44	0.47 ± 0.38	1.18 ± 0.37	1.70 ± 0.51	0.96 ± 0.43	1.82 ± 0.21	2.71 ± 0.46
Group 2	0.56 ± 0.29	0.30 ± 0.18	0.18 ± 0.15	0.72 ± 0.21	2.30 ± 0.49	0.71 ± 0.21	0.31 ± 0.16	2.45 ± 0.45
Group 3	1.17 ± 0.55	1.49 ± 0.51	2.44 ± 0.67	3.21 ± 0.40	1.22 ± 0.21	0.34 ± 0.23	0.37 ± 0.26	1.36 ± 0.17
Group 4	0.49 ± 0.34	0.24 ± 0.24	1.78 ± 0.29	1.90 ± 0.28	0.49 ± 0.25	0.18 ± 0.12	0.33 ± 0.32	0.68 ± 0.29
Group 5	0.41 ± 0.27	0.39 ± 0.19	0.46 ± 0.21	0.80 ± 0.22	0.54 ± 0.22	0.40 ± 0.21	0.30 ± 0.21	0.80 ± 0.19

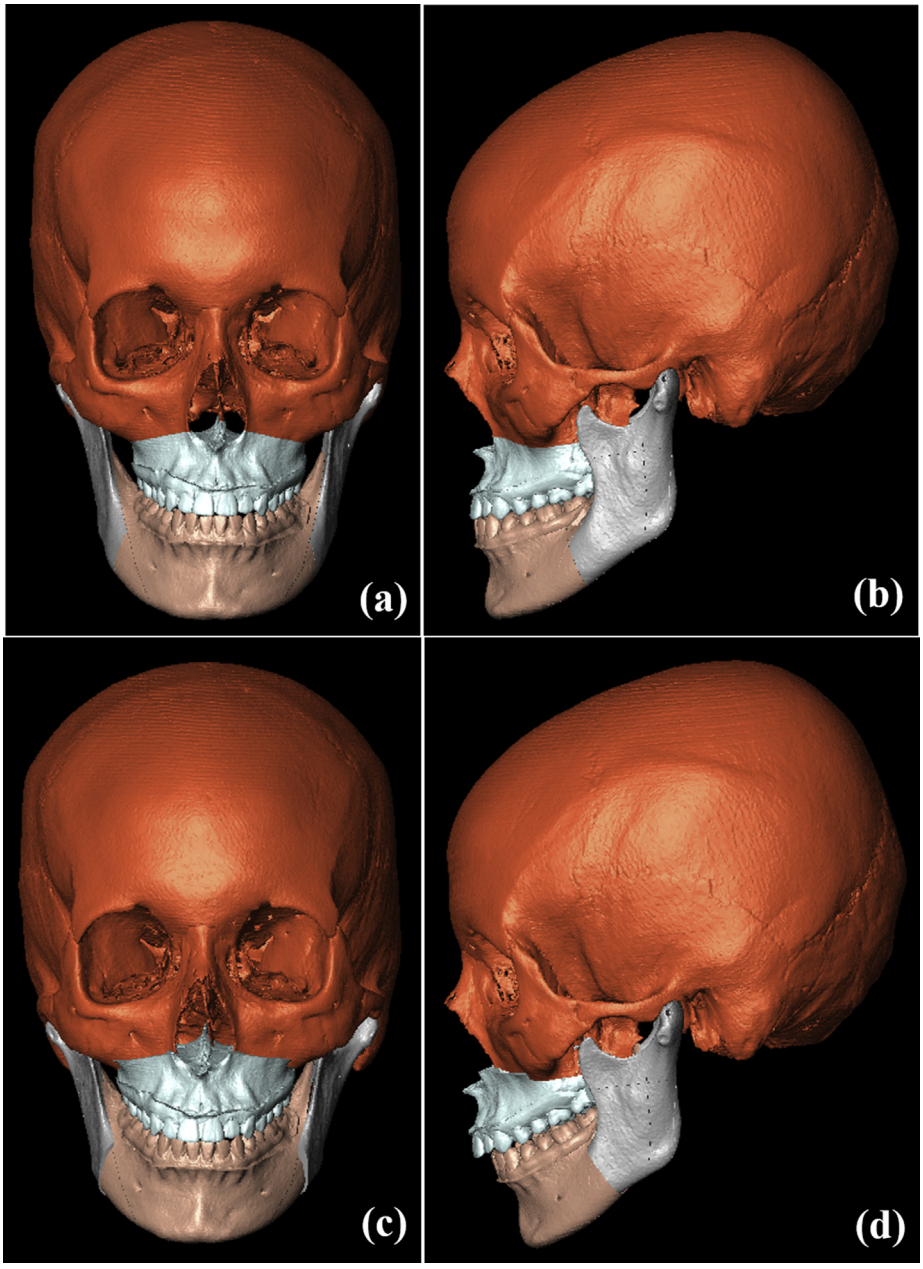

Fig. 5. Virtual maxillary, mandibular distal, and mandibular proximal segment (MPS) models in 3D coronal (a) and sagittal (b) views before planning, and their simulated models in coronal (c) and sagittal (d) views after planning.

differences at the three condylar landmarks differed significantly from that at the landmark of the angle of the mandible ($p < 0.05$).

4. Discussion

To date, the relationship between positional displacements of the condyle after orthognathic surgery and TMJ function remains uncertain (Nova et al., 2017). The purpose of repositioning the MPS during orthognathic surgery has been to guarantee the stability of the surgery, reduce the harmful effects on the TMJ, and enhance patients' masticatory function (Costa et al., 2008). When mandibular autorotation occurs, it creates a difference between the condylar center and the mandibular rotation center, and differences in the range of 10–20 mm can have a clinically significant effect on the outcome of orthognathic surgery and lead to substantial errors in the position of the maxilla (Nattestad et al., 1992). Minimizing mandibular autorotation is also important for obtaining stable skeletal and occlusal results after orthognathic surgery, and preventing temporomandibular disorders (Nattestad et al., 1992; Chapuis et al., 2007).

To move the MPS as close as possible to its preoperative position, previous researchers have introduced several techniques, such as using face bow recording methods (Chow et al., 1985; Zizelmann et al., 2012), templates (Harada et al., 1994; Stoelinga et al., 2003; Abou-ElFetouh et al., 2011), splints (Landes et al., 2003), and condylar positioning devices (Gerressen et al., 2006, 2007). However, the face bow methods could not reliably express the anatomic reference planes (Zizelmann et al., 2012). The use of templates seemed to be a solution to the problems of the face bow methods, but the elasticity and strength of the template material significantly

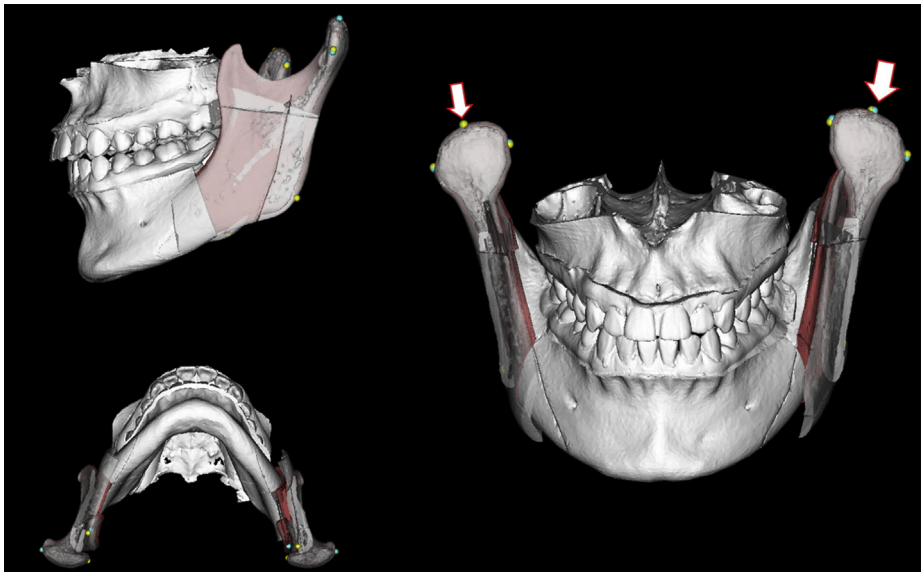

Fig. 6. Visualization of the pre-planning (in gray) and simulated (in red) MPS models, and the pre-planning (indicated in yellow by a thin arrow) and simulated (in cyan, thick arrow) positions of three landmarks at the condyle and one at the angle of the mandible.

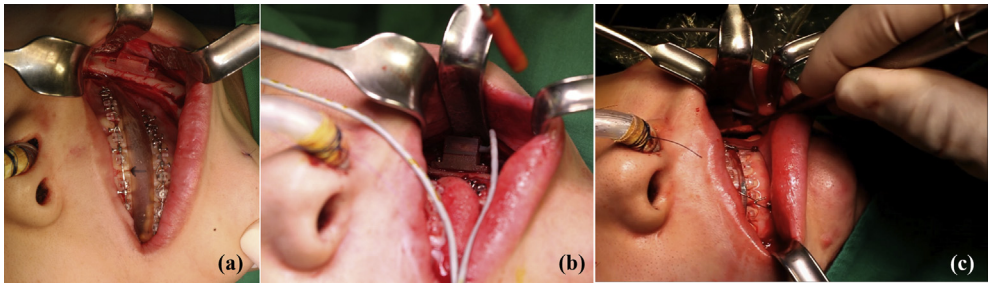

Fig. 7. The frame installed on the patient's MPS (a) was attached with the tracking tool by insertion (b), and the patient's MPS was repositioned to the planned position (c).

affected surgical outcomes, so the surgical plan could not be reproduced accurately (Abou-ElFetouh et al., 2011). Repositioning the MPS using splints was introduced to overcome the problems with the template methods. However, the splint could not effectively prevent autorotation of the mandible (Ellis, 1994). The basic idea of using a condylar positioning device for repositioning the MPS was reasonable and inventive, but an experienced surgeon could manually provide good surgical results with similar accuracy (Gerressen et al., 2006). Another significant limitation of those methods is that the positional relationship between the condyle and fossa could not be recognized in real time during surgery.

With advances in medical imaging and 3D positional tracking technology, image-guided surgery methods, including preoperative planning and planning transfer, have been used in the oral and maxillofacial field (Xia et al., 2001; Chapuis et al., 2007; Bell et al., 2009; Bell, 2010, 2011; Ghanai et al., 2010; Frisardi et al., 2011; Centenero et al., 2012; Coppen et al., 2013; Polley et al., 2013; Farrell et al., 2014; Kim et al., 2014; Bobek et al., 2015; Gander et al., 2015; Uechi et al., 2015). Generally, image-guided surgery has been used in orthognathic surgery for maxillary and mandibular positioning, and in dental implant surgery (Nijmeh et al., 2005; Strong et al., 2008; Eggers et al., 2009; Zhang et al., 2011, 2012; Seeberger et al., 2012; Kim et al., 2013, 2014; Li et al., 2014; Lee et al., 2016). In our previous studies, we developed an image-guided orthognathic surgery system for virtual planning and transfer (Kim et al., 2014). We also developed a complex model-guided orthognathic surgery system using virtual models integrated with high-resolution, optically scanned dentition (Lee et al., 2016). To date, those image-guided surgery methods have focused mainly on repositioning the maxillary and mandibular distal bone segments.

Most image-guided surgery systems have been based on an optical tracking system that tracks the surgical target using infrared light. Although those systems guarantee a high degree of tracking accuracy, their line-of-sight requirement between the optical tracking tools and the camera are an important limitation, especially in delicate surgical environments. In addition, the relatively large and heavy tracking tools are difficult to use in minimally invasive surgery or proximal segment repositioning (Bettega et al., 1996). Previous studies have demonstrated the feasibility of applying electromagnetic tracking to orthognathic surgery (Berger et al., 2015; Lutz et al., 2015; Nova et al., 2017). In one previous study, an electromagnetic tracking-based navigation system was applied to repositioning of the MPS after mandibular osteotomy (Berger et al., 2018). However, that electromagnetic tracking tool could not be repeatedly separated and attached according to the procedural needs of MPS surgery because the tracking tool itself was fixed firmly to the bone surface using screws. The tracking tool cable could thus interfer with the surgeon's line of sight, and restrict access, whilst potential damage to the cable from the sharp surgical instruments used to perform osteotomies and bone removal could increase surgical time and effort, and cause iatrogenic accidents (Berger et al., 2018).

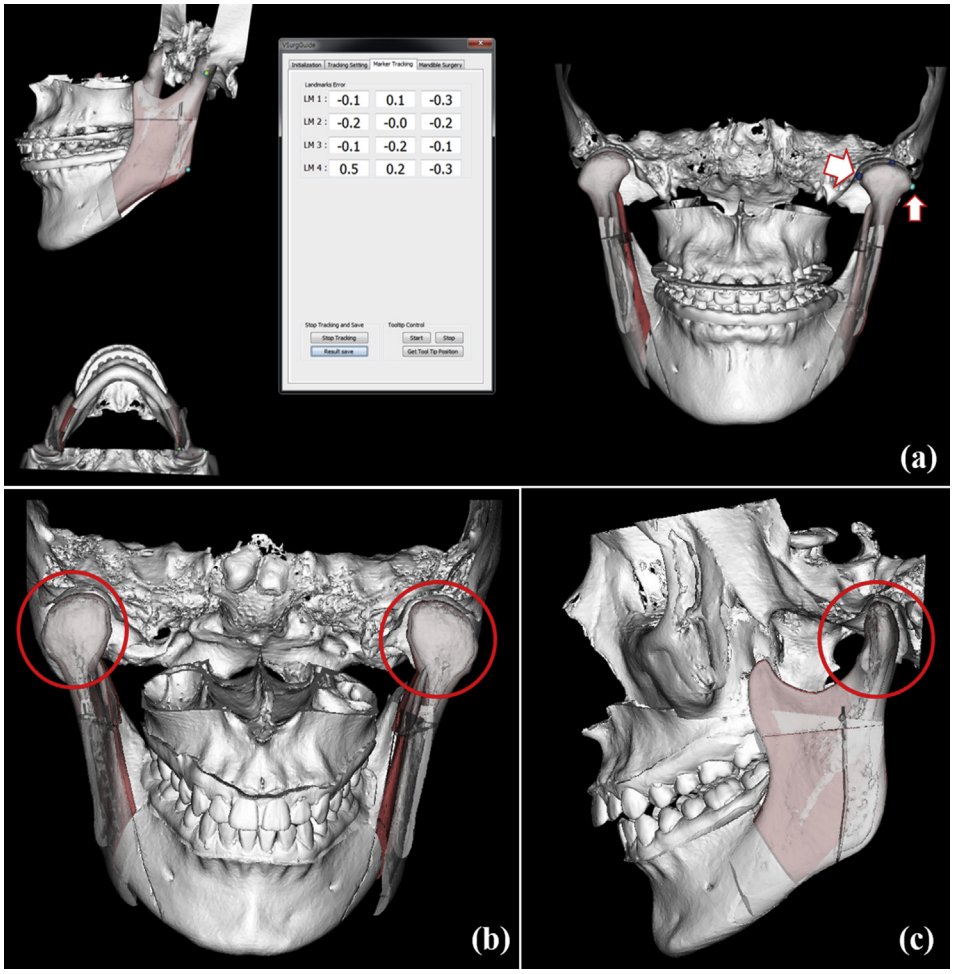

Fig. 8. Visualization of the positional deviations between the current (close position indicated in blue by a thick arrow) and simulated (in cyan, thin arrow) positions of the landmarks (a), and visualization of the 3D condyle–fossa positional relationship in coronal (b) and sagittal (c) views.

Table 3
Absolute differences in the *x*, y, and *z* axes and root mean square (RMS) differences between the simulated and intraoperative models, and between the simulated and postoperative models at three landmarks on the condyle (1, 2, 3) and one on the angle of the mandible (4).

Landmarks	Intraoperative model (mm)			Postoperative model (mm)		
	x	*y*	*z*	*x*	*y*	*z*
1	1.57	0.50	1.51	0.94	0.08	1.40
2	1.66	0.21	0.83	0.47	0.69	1.65
3	0.89	0.36	0.33	1.42	0.71	1.42
4	1.92	1.50	1.45	1.88	2.76	1.36
Mean (1, 2,3)	1.37 ± 0.42	0.36 ± 0.15	0.89 ± 0.59	0.94 ± 0.48	0.49 ± 0.36	1.49 ± 0.14
Mean (1, 2, 3, 4)	1.51 ± 0.44	0.64 ± 0.58	1.03 ± 0.56	1.18 ± 0.61	1.06 ± 1.17	1.46 ± 0.13
RMS (1, 2, 3)	1.71 ± 0.63			1.89 ± 0.22		
RMS (1, 2, 3, 4)	1.94 ± 0.76			2.32 ± 0.88		

For our study, we developed a frame that allowed us to attach and separate the electromagnetic tracking tool from the MPS bone. Because only part of the frame was fixed to the patient's MPS by surgical screws, the electromagnetic tracking tool could easily be inserted and removed as needed. The frame occupied a small area and could be fixed onto any part of the MPS. As a result, the electromagnetic tracking tool could be attached to and separated from the MPS bone repeatedly during surgery whilst maintaining the same geometrical relationship, allowing the surgeon to perform various osteotomies and bone removal conveniently and accurately without interference by the cable connecting the tracking tool.

An essential element of image-guided surgery is accurate registration for matching the patient's image space with their physical space. Generally, the registration process is performed through the matching of corresponding points between the two spaces (Zhang et al., 2011, 2012; Kim et al., 2013, 2014; Lee et al., 2016), or through a surface matching method using spatial information about the surface of the patient's anatomical structure (Besl et al., 1992; Soteriou et al., 2016). Registration accuracy decreases as the distance between the position of the tracking target and the location of the registration fiducials increases (Soteriou et al., 2016). Therefore, the accuracy of image-guided surgery for structures in

deep parts of the body, such as the MPS, can be seriously reduced by registration that uses points far from the structure.

In this study, the point-to-point registration between the patient's image and physical spaces was performed using corresponding fiducial points on the registration body. The physical locations of the fiducials on the registration body were made as close as possible to the posterior mandible. We used the fiducial groups showing the highest registration accuracy in the phantom study. In addition, we were able to measure the positions of the fiducials on the registration body preoperatively and use them intraoperatively because the registration body (with a tracking tool) and the patient splint were always in the same positional relationship. Therefore, intraoperative registration was accurate and immediate because it could use the optimal preoperative registration result, saving the surgeon time and labor during the operation.

During repositioning, the current, augmented MPS model was visualized with respect to the simulated MPS model in real time, and the intraoperative positions of the landmarks were visualized on the MPS surface model. Three-dimensional deviation errors between the intraoperative and simulated positions of the landmarks on the MPS were calculated continuously and visualized quantitatively without applying an electromagnetic pointing tool directly to the MPS bone surface (Kim et al., 2014; Lee et al., 2016). In addition, our method provided augmented 3D coronal and sagittal views of the positional relationship between the condyle and the glenoid fossa. Therefore, the 3D position of the condyle and its landmarks were visualized quantitatively with respect to the glenoid fossa and localized continuously in real time, allowing the surgeon to recognize the 3D condyle–fossa positional relationship accurately during the MPS repositioning. As a result, the surgeon could intuitively and easily recognize the current 3D position of the condyle with respect to the simulated position and determine the directions and displacements needed to move the MPS into the target position.

Immediately after repositioning the MPS using the image guidance, the mean RMS difference between the landmark positions established in the planning and from the intraoperative guidance was 1.94 ± 0.76 mm at four MPS landmarks, and the mean RMS difference was 1.71 ± 0.63 mm at three condylar landmarks. By the time of the postoperative evaluation, the mean RMS difference between the positions acquired by the planning and the postoperative CT was 2.32 ± 0.88 mm at the same MPS landmarks, and the mean RMS difference was 1.89 ± 0.22 mm at three condylar landmarks. The condylar landmark results showed higher accuracy than previously achieved in repositioning the condyle of the MPS (Berger et al., 2018). In a previous study, the differences between the pre- and postoperative positions of the defined center point of the proximal segment were 0.27, 0.01, and −2.27 mm on the *x*, *y*, and *z* axes, respectively (Berger et al., 2018). The accuracy at the condylar landmarks for repositioning the condyle in the fossa showed a clinically acceptable level of accuracy (under 2 mm) by our method (Hassfeld et al., 2001).

Our image-guided surgery method for MPS repositioning requires further development to increase its accuracy, by reducing technical errors from the tracking devices, imaging errors from the modalities, registration errors, application errors, and human error (Widmann et al., 2009).

5. Conclusion

We have developed an augmented, model-guided, surgical method for MPS repositioning with high accuracy and convenience in clinical application. The registration process uses optimal fiducials on the registration body and shows high accuracy in repositioning the MPS. The MPS tracking tool can be attached to and separated from the MPS bone repeatedly and conveniently, for the surgeon to perform the required osteotomies and bone removal. As a result, the surgeon can perform the MPS repositioning conveniently and accurately, based on real-time information about the 3D condyle positional relationship with respect to the glenoid fossa from augmented and simulated models and landmarks. In a future study, we will improve the accuracy of the augmented model-guided system based on electromagnetic tracking, and apply it to more patients with maxillofacial deformities.

Acknowledgements

This work was supported by the Technology Innovation Program (10063389), funded by the Ministry of Trade, Industry & Energy (MOTIE), Korea.

Appendix A. Supplementary data

Supplementary data to this article can be found online at https://doi.org/10.1016/j.jcms.2018.10.016.

References

Abou-ElFetouh A, Barakat A, Abdel-Ghany K: Computer-guided rapid-prototyped templates for segmental mandibular osteotomies: a preliminary report. Int J Med Robot Comp 7: 187–192, 2011

Bell RB: Computer planning and intraoperative navigation in cranio-maxillofacial surgery. Oral Maxillofac Surg Clin 22: 135–156, 2010

Bell RB: Computer planning and intraoperative navigation in orthognathic surgery. J Oral Maxillofac Surg 69: 592–605, 2011

Bell RB, Markiewicz MR: Computer-assisted planning, stereolithographic modeling, and intraoperative navigation for complex orbital reconstruction: a descriptive study in a preliminary cohort. J Oral Maxillofac Surg 67: 2559–2570, 2009

Berger M, Kallus S, Nova I, Ristow O, Eisenmann U, Dickhaus H, Kuhle R, Hoffmann J, Seeberger R: Approach to intraoperative electromagnetic navigation in orthognathic surgery: a phantom skull based trial. J Cranio Maxillofac Surg 43: 1731–1736, 2015

Berger M, Nova I, Kallus S, Ristow O, Eisenmann U, Dickhaus H, Engel M, Freudlsperger C, Hoffmann J, Seeberger R: Electromagnetic navigated condylar positioning after high oblique sagittal split osteotomy of the mandible: a guided method to attain pristine temporomandibular joint conditions. Oral Surg Oral Med Oral Pathol Oral Radiol 125: 407–414, 2018

Besl PJ, Mckay ND: A method for registration of 3-D shapes. IEEE Trans Pattern Anal 14: 239–256, 1992

Bettega G, Cinquin P, Lebeau J, Raphael B: Computer-assisted orthognathic surgery: clinical evaluation of a mandibular condyle repositioning system. J Oral Maxillofac Surg 60: 27–34, 2002

Bettega G, Dessenne V, Raphael B, Cinquin P: Computer-assisted mandibular condyle positioning in orthognathic surgery. J Oral Maxillofac Surg 54: 553–558, 1996

Bettega G, Leitner F: Computer assisted orthognathic surgery: condyle repositioning. Rev Stomatol Chir 114: 205–210, 2013

Bobek SL: Applications of navigation for orthognathic surgery. Oral Maxil Surg Clin 26: 587–598, 2014

Bobek S, Farrell B, Choi C, Farrell B, Weimer K, Tucker M: Virtual surgical planning for orthognathic surgery using digital data transfer and an intraoral fiducial marker: the Charlotte method. J Oral Maxillofac Surg 73: 1143–1158, 2015

Centenero SAH, Hernandez-Alfaro F: 3D planning in orthognathic surgery: CAD/CAM surgical splints and prediction of the soft and hard tissues results — our experience in 16 cases. J Cranio Maxillofac Surg 40: 162–168, 2012

Chapuis J, Schramm A, Pappas I, Hallermann W, Schwenzer-Zimmerer K, Langlotz F, Caversaccio M: A new system for computer-aided preoperative planning and intraoperative navigation during corrective jaw surgery. IEEE Trans Inf Technol B 11: 274–287, 2007

Chow TW, Clark RKF, Cooke MS: Errors in mounting maxillary casts using face-bow records as a result of an anatomical variation. J Dent 13: 277–282, 1985

Coppen C, Weijs W, Berge SJ, Maal TJJ: Oromandibular reconstruction using 3D planned triple template method. J Oral Maxillofac Surg 71: E243–E247, 2013

Costa F, Robiony M, Toro C, Sembronio S, Polini F, Politi M: Condylar positioning devices for orthognathic surgery: a literature review. Oral Surg Oral Med Oral Pathol Oral Radiol 106: 179–190, 2008

Eggers G, Muhling J, Hofele C: Clinical use of navigation based on cone-beam computer tomography in maxillofacial surgery. Brit J Oral Maxillofac Surg 47: 450–454, 2009

Ellis E: Condylar positioning devices for orthognathic surgery — are they necessary? J Oral Maxillofac Surg 52: 536–552, 1994
Ellis E, Hinton RJ: Histologic examination of the temporomandibular joint after mandibular advancement with and without rigid fixation — an experimental investigation in adult Macaca mulatta. J Oral Maxillofac Surg 49: 1316–1327, 1991
Epker BN, Wylie GA: Control of the condylar-proximal mandibular segments after sagittal split osteotomies to advance the mandible. Oral Surg Oral Med Oral Pathol Oral Radiol Endodontics 62: 613–617, 1986
Farrell BB, Franco PB, Tucker MR: Virtual surgical planning in orthognathic surgery. Oral Maxillofac Surg Clin 26: 459–473, 2014
Frisardi G, Chessa G, Barone S, Paoli A, Razionale A, Frisardi F: Integration of 3D anatomical data obtained by CT imaging and 3D optical scanning for computer aided implant surgery. BMC Med Imag 11, 2011
Gander T, Bredell M, Eliades T, Rucker M, Essig H: Splintless orthognathic surgery: a novel technique using patient-specific implants (PSI). J Cranio Maxillofac Surg 43: 319–322, 2015
Gerressen M, Stockbrink G, Smeets RF, Riediger D, Gbassemi A: Skeletal stability following bilateral sagittal split osteotomy (BSSO) with and without condylar positioning device. J Oral Maxillofac Surg 65: 1297–1302, 2007
Gerressen M, Zadeh MD, Stockbrink G, Riediger D, Ghassemi A: The functional long-term results after bilateral sagittal split osteotomy (BSSO) with and without a condylar positioning device. J Oral Maxillofac Surg 64: 1624–1630, 2006
Ghanai S, Marmulla R, Wiechnik J, Muhling J, Kotrikova B: Computer-assisted three-dimensional surgical planning: 3D virtual articulator: technical note. Int J Oral Maxillofac Surg 39: 75–82, 2010
Harada K, Okada Y, Nagura H, Enomoto S: A new repositioning system for the proximal segment in sagittal split ramus osteotomy of the mandible. Int J Oral Maxillofac Surg 23: 71–73, 1994
Hassfeld S, Muhling J: Computer assisted oral and maxillofacial surgery — a review and an assessment of technology. Int J Oral Maxillofac Surg 30: 2–13, 2001
Hoppenreijs TJM, Stoelinga PJW, Grace KL, Robben CMG: Long-term evaluation of patients with progressive condylar resorption following orthognathic surgery. Int J Oral Maxillofac Surg 28: 411–418, 1999
Hu J, Wang DZ, Zou SJ: Effects of mandibular setback on the temporomandibular joint: a comparison of oblique and sagittal split ramus osteotomy. J Oral Maxillofac Surg 58: 375–380, 2000
Hwang SJ, Haers VE, Seifert B, Sailer HF: Non-surgical risk factors for condylar resorption after orthognathic surgery. J Cranio Maxillofac Surg 32: 103–111, 2004
Kim DS, Woo SY, Yang HJ, Huh KH, Lee SS, Heo MS, Choi SC, Hwang SJ, Yi WJ: An integrated orthognathic surgery system for virtual planning and image-guided transfer without intermediate splint. J Cranio Maxillofac Surg 42: 2010–2017, 2014
Kim SH, Kim DS, Huh KH, Lee SS, Heo MS, Choi SC, Hwang SJ, Yi WJ: Direct and continuous localization of anatomical landmarks for image-guided orthognathic surgery. Or Surg Or Med Or Pa 116: 402–410, 2013
Komori E, Aigase K, Sugisaki M, Tanabe H: Cause of early skeletal relapse after mandibular setback. Am J Orthod Dentofac 95: 29–36, 1989
Landes CA, Sterz M: Proximal segment positioning in bilateral sagittal split osteotomy: intraoperative controlled positioning by a positioning splint. J Oral Maxillofac Surg 61: 1423–1431, 2003
Lee SJ, Woo SY, Huh KH, Lee SS, Heo MS, Choi SC, Han JJ, Yang HJ, Hwang SJ, Yi WJ: Virtual skeletal complex model- and landmark-guided orthognathic surgery system. J Cranio Maxillofac Surg 44: 557–568, 2016
Li B, Zhang L, Sun H, Shen SGF, Wang XD: A new method of surgical navigation for orthognathic surgery: optical tracking guided free- hand repositioning of the maxillomandibular complex. J Craniofac Surg 25: 406–411, 2014
Lutz JC, Nicolau S, Agnus V, Bodin F, Wilk A, Bruant-Rodier C, Remond Y, Soler L: A novel navigation system for maxillary positioning in orthognathic surgery: preclinical evaluation. J Cranio Maxillofac Surg 43: 1723–1730, 2015
Marmulla R, Muhling J: Computer-assisted condyle positioning in orthognathic surgery. J Oral Maxillofac Surg 65: 1963–1968, 2007
Naether S, Buck U, Campana L, Breitbeck R, Thali M: The examination and identification of bite marks in foods using 3D scanning and 3D comparison methods. Int J Leg Med 126: 89–95, 2012
Nattestad A, Vedtofte P: Mandibular autorotation in orthognathic surgery — a new method of locating the center of mandibular rotation and determining its consequence in orthognathic surgery. J Cranio Maxillofac Surg 20: 163–170, 1992
Nijmeh AD, Goodger NM, Hawkes D, Edwards PJ, McGurk M: Image-guided navigation in oral and maxillofacial surgery. Brit J Oral Maxillofac Surg 43: 294–302, 2005
Nkenke E, Zachow S, Benz M, Maier T, Veit K, Kramer M, Benz S, Hausler G, Neukam FW, Lell M: Fusion of computed tomography data and optical 3D images of the dentition for streak artefact correction in the simulation of orthognathic surgery. Dentomaxillofac Rad 33: 226–232, 2004
Nova I, Kallus S, Berger M, Ristow O, Eisenmann U, Freudlsperger C, Hoffmann J, Dickhaus H: Computer assisted positioning of the proximal segment after sagittal split osteotomy of the mandible: preclinical investigation of a novel electromagnetic navigation system. J Cranio Maxillofac Surg 45: 748–754, 2017
Panula K, Somppi M, Finne K, Oikarinen K: Effects of orthognathic surgery on temporomandibular joint dysfunction — a controlled prospective 4-year follow-up study. Int J Oral Maxillofac Surg 29: 183–187, 2000
Politi M, Costa F, Cian R, Polini F, Robiony M: Stability of skeletal class III malocclusion after combined maxillary and mandibular procedures: rigid internal fixation versus wire osteosynthesis of the mandible. J Oral Maxillofac Surg 62: 169–181, 2004
Polley JW, Figueroa AA: Orthognathic positioning system: intraoperative system to transfer virtual surgical plan to operating field during orthognathic surgery. J Oral Maxillofac Surg 71: 911–920, 2013
Savoldelli C, Chamorey E, Bettega G: Computer-assisted teaching of bilateral sagittal split osteotomy: learning curve for condylar positioning. Plos One 13, 2018
Seeberger R, Kane G, Hoffmann J, Eggers G: Accuracy assessment for navigated maxillo-facial surgery using an electromagnetic tracking device. J Cranio Maxillofac Surg 40: 156–161, 2012
Sohmura T, Nagao M, Sakai M, Wakabayashi K, Kojima T, Kinuta S, Nakamura T, Takahashi J: High-resolution 3-D shape integration of dentition and face measured by new laser scanner. IEEE Trans Med Imag 23: 633–638, 2004
Soteriou E, Grauvogel J, Laszig R, Grauvogel TD: Prospects and limitations of different registration modalities in electromagnetic ENT navigation. Eur Arch Oto-Rhino-L 273: 3979–3986, 2016
Stoelinga PJW, Borstlap WA: The fixation of sagittal split osteotomies with miniplates: the versatility of a technique. J Oral Maxillofac Surg 61: 1471–1476, 2003
Strong EB, Rafii A, Holhweg-Majert B, Fuller SC, Metzger MC: Comparison of 3 optical navigation systems for computer-aided maxillofacial surgery. Arch Otolaryngol 134: 1080–1084, 2008
Uechi J, Okayama M, Shibata T, Muguruma T, Hayashi K, Endo K, Mizoguchi I: A novel method for the 3-dimensional simulation of orthognathic surgery by using a multimodal image-fusion technique. Am J Orthod Dentofac 130: 786–798, 2006
Uechi J, Tsuji Y, Konno M, Hayashi K, Shibata T, Nakayama E, Mizoguchi I: Generation of virtual models for planning orthognathic surgery using a modified multimodal image fusion technique. Int J Oral Maxillofac Surg 44: 462–469, 2015
Widmann G, Stoffner R, Bale R: Errors and error management in image-guided craniomaxillofacial surgery. Oral Surg Oral Med Oral Pathol Oral Radiol 107: 701–715, 2009
Wolford LM, Reiche-Fischel O, Mehra P: Changes in temporomandibular joint dysfunction after orthognathic surgery. J Oral Maxillofac Surg 61: 655–660, 2003
Xia J, Ip HHS, Samman N, Wong HTF, Gateno J, Wang DF, Yeung RWK, Kot CSB, Tideman H: Three-dimensional virtual-reality surgical planning and soft-tissue prediction for orthognathic surgery. IEEE Trans Inf Technol B 5: 97–107, 2001
Zhang WB, Wang CH, Shen GF, Wang XD, Cai M, Gui HJ, Liu YC, Yang DL: A novel device for preoperative registration and automatic tracking in cranio-maxillofacial image guided surgery. Comput Aided Surg 17: 259–267, 2012
Zhang WB, Wang CH, Yu HB, Liu YC, Shen GF: Effect of fiducial configuration on target registration error in image-guided cranio-maxillofacial surgery. J Cranio Maxillofac Surg 39: 407–411, 2011
Zizelmann C, Hammer B, Gellrich NC, Schwestka-Polly R, Rana M, Bucher P: An evaluation of face-bow transfer for the planning of orthognathic surgery. J Oral Maxillofac Surg 70: 1944–1950, 2012